

# Enhanced performance of Cr,Yb:YAG microchip laser by bonding Yb:YAG crystal

Ying Cheng, Jun Dong,\* and Yingying Ren

Department of Electronics Engineering, School of Information Science and Technology, Xiamen University, Xiamen 361005, China  
\*jddong@xmu.edu.cn

**Abstract:** Highly efficient, laser-diode pumped Yb:YAG/Cr,Yb:YAG self-Q-switched microchip lasers by bonding Yb:YAG crystal have been demonstrated for the first time to our best knowledge. The effect of transmission of output coupler ( $T_{oc}$ ) on the enhanced performance of Yb:YAG/Cr,Yb:YAG microchip lasers has been investigated and found that the best laser performance was achieved with  $T_{oc} = 50\%$ . Slope efficiency of over 38% was achieved. Average output power of 0.8 W was obtained at absorbed pump power of 2.5 W; corresponding optical-to-optical efficiency of 32% was obtained. Laser pulses with pulse width of 1.68 ns, pulse energy of 12.4  $\mu$ J, and peak power of 7.4 kW were obtained. The lasers oscillated in multi-longitudinal modes. The wide separation of longitudinal modes was attributed to the mode selection by combined etalon effect of Cr,Yb:YAG, Yb:YAG thin plates and output coupler. Stable periodical pulse trains at different pump power levels have been observed owing to the longitudinal modes coupling and competition.

©2012 Optical Society of America

**OCIS codes:** (140.3380) Laser materials; (140.3480) Lasers, diode-pumped; (140.3540) Lasers, Q-switched; (140.3580) Lasers, solid-state; (140.3615) Lasers, ytterbium; (140.5680) Rare earth and transition metal solid-state lasers.

---

## References and links

1. H. Kofler, J. Tauer, G. Tartar, K. Iskra, J. Klausner, G. Herdin, and E. Wintner, "An innovative solid-state laser for engine ignition," *Laser Phys. Lett.* **4**(4), 322–327 (2007).
2. J. J. Zayhowski, "Microchip lasers," *Opt. Mater.* **11**(2-3), 255–267 (1999).
3. J. J. Zayhowski, "Q-switched microchip lasers find real-world application," *Laser Focus World* **35**, 129–136 (1999).
4. P. Wang, S. Zhou, K. K. Lee, and Y. C. Chen, "Picosecond laser pulse generation in a monolithic self-Q-switched solid-state laser," *Opt. Commun.* **114**(5-6), 439–441 (1995).
5. J. Dong, P. Deng, Y. Lu, Y. Zhang, Y. Liu, J. Xu, and W. Chen, "Laser-diode-pumped Cr<sup>4+</sup>, Nd<sup>3+</sup>:YAG with self-Q-switched laser output of 1.4 W," *Opt. Lett.* **25**(15), 1101–1103 (2000).
6. J. Dong, P. Deng, Y. Liu, Y. Zhang, G. Huang, and F. Gan, "Performance of the self-Q-switched Cr,Yb:YAG laser," *Chin. Phys. Lett.* **19**(3), 342–344 (2002).
7. D. S. Sumida and T. Y. Fan, "Effect of radiation trapping on fluorescence lifetime and emission cross section measurements in solid-state laser media," *Opt. Lett.* **19**(17), 1343–1345 (1994).
8. T. Y. Fan, "Heat generation in Nd:YAG and Yb:YAG," *IEEE J. Quantum Electron.* **29**(6), 1457–1459 (1993).
9. H. W. Bruesselbach, D. S. Sumida, R. A. Reeder, and R. W. Byren, "Low-heat high-power scaling using InGaAs-diode-pumped Yb:YAG lasers," *IEEE J. Sel. Top. Quantum Electron.* **3**(1), 105–116 (1997).
10. J. Dong, M. Bass, Y. Mao, P. Deng, and F. Gan, "Dependence of the Yb<sup>3+</sup> emission cross section and lifetime on the temperature and concentration in ytterbium aluminum garnet," *J. Opt. Soc. Am. B* **20**(9), 1975–1979 (2003).
11. F. D. Patel, E. C. Honea, J. Speth, S. A. Payne, R. Hutcheson, and R. Equall, "Laser demonstration of Yb<sub>3</sub>Al<sub>5</sub>O<sub>12</sub> (YAG) and materials properties of highly doped Yb:YAG," *IEEE J. Quantum Electron.* **37**(1), 135–144 (2001).
12. J. Kawanaka, Y. Takeuchi, A. Yoshida, S. J. Pearce, R. Yasuhara, T. Kawashima, and H. Kan, "Highly efficient cryogenically-cooled Yb:YAG laser," *Laser Phys.* **20**(5), 1079–1084 (2010).
13. A. Giesen and J. Speiser, "Fifteen years of work on thin-disk lasers: results and scaling laws," *IEEE J. Sel. Top. Quantum Electron.* **13**(3), 598–609 (2007).
14. C. Stewen, K. Contag, M. Larionov, A. Giesen, and H. Hugel, "A 1-kW CW Thin Disc laser," *IEEE J. Sel. Top. Quantum Electron.* **6**(4), 650–657 (2000).
15. A. G. Wang, Y. Li, L., and F. X. H., "Quasi-three-level thin-disk laser at 1024 nm based on diode-pumped Yb:YAG crystal," *Laser Phys. Lett.* **8**, 508–511 (2011).

16. E. C. Honea, R. J. Beach, S. C. Mitchell, J. A. Skidmore, M. A. Emanuel, S. B. Sutton, S. A. Payne, P. V. Avizonis, R. S. Monroe, and D. G. Harris, "High-power dual-rod Yb:YAG laser," *Opt. Lett.* **25**(11), 805–807 (2000).
17. J. Dong, A. Shirakawa, K. Ueda, J. Xu, and P. Deng, "Efficient laser oscillation of Yb:Y<sub>3</sub>Al<sub>5</sub>O<sub>12</sub> single crystal grown by temperature gradient technique," *Appl. Phys. Lett.* **88**(16), 161115 (2006).
18. J. Dong, A. Shirakawa, K. Ueda, H. Yagi, T. Yanagitani, and A. A. Kaminskii, "Efficient Yb<sup>3+</sup>:Y<sub>3</sub>Al<sub>5</sub>O<sub>12</sub> ceramic microchip lasers," *Appl. Phys. Lett.* **89**(9), 091114 (2006).
19. T. S. Rutherford, W. M. Tulloch, E. K. Gustafson, and R. L. Byer, "Edge-pumped quasi-three-level slab lasers: design and power scaling," *IEEE J. Quantum Electron.* **36**(2), 205–219 (2000).
20. J. Dong, P. Deng, Y. Liu, Y. Zhang, J. Xu, W. Chen, and X. Xie, "Passively-Q-switched Yb:YAG laser with Cr<sup>4+</sup>:YAG as a saturable absorber," *Appl. Opt.* **40**(24), 4303–4307 (2001).
21. J. Dong, P. Deng, and J. Xu, "The growth of Cr<sup>4+</sup>, Yb<sup>3+</sup>:yttrium aluminum garnet(YAG) crystal and its absorption spectra properties," *J. Cryst. Growth* **203**(1-2), 163–167 (1999).
22. J. Dong and P. Deng, "The effect of Cr concentration on emission cross section and fluorescence lifetime in Cr,Yb:YAG crystal," *J. Lumin.* **104**(1-2), 151–158 (2003).
23. J. Dong, A. Shirakawa, S. Huang, Y. Feng, T. Takaichi, M. Musha, K. Ueda, and A. A. Kaminskii, "Stable laser-diode pumped microchip sub-nanosecond Cr,Yb:YAG self-Q-switched laser," *Laser Phys. Lett.* **2**(8), 387–391 (2005).
24. H. Eilers, U. Hömmerich, S. M. Jacobsen, W. M. Yen, K. R. Hoffman, and W. Jia, "Spectroscopy and dynamics of Cr<sup>4+</sup>:Y<sub>3</sub>Al<sub>5</sub>O<sub>12</sub>," *Phys. Rev. B Condens. Matter* **49**(22), 15505–15513 (1994).
25. R. Feldman, Y. Shimony, and Z. Burshtein, "Dynamics of chromium ion valence transformations in Cr,Ca:YAG crystals used as laser gain and passive Q-switching media," *Opt. Mater.* **24**(1-2), 333–344 (2003).
26. J. Y. Zhou, J. Ma, J. Dong, Y. Cheng, K. Ueda, and A. A. Kaminskii, "Efficient, nanosecond self-Q-switched Cr,Yb:YAG lasers by bonding Yb:YAG crystal," *Laser Phys. Lett.* **8**(8), 591–597 (2011).
27. J. Dong, J. Ma, Y. Cheng, Y. Y. Ren, K. Ueda, and A. A. Kaminskii, "Comparative study on enhancement of self-Q-switched Cr,Yb:YAG lasers by bonding Yb:YAG ceramic and crystal," *Laser Phys. Lett.* **8**(12), 845–852 (2011).
28. W. Koehner, *Solid State Laser Engineering* (Springer-Verlag, Berlin, 1999).
29. J. Dong and P. Deng, "Temperature dependent emission cross-section and fluorescence lifetime of Cr,Yb:YAG crystals," *J. Phys. Chem. Solids* **64**(7), 1163–1171 (2003).
30. J. Dong, "Numerical modeling of CW-pumped repetitively passively Q-switched Yb:YAG lasers with Cr:YAG as saturable absorber," *Opt. Commun.* **226**(1-6), 337–344 (2003).
31. J. J. Degnan, "Optimization of passively Q-switched lasers," *IEEE J. Quantum Electron.* **31**(11), 1890–1901 (1995).

---

## 1. Introduction

Laser-diode pumped passively Q-switched solid-state lasers with Cr<sup>4+</sup>:YAG as saturable absorber are compact and robust lasers with high pulse energies and peak powers in a diffraction-limited output beam, and have many applications such as remote sensing, range finders, pollution detection, lidar, material processing, medical systems, laser ignition, and so on [1–3]. Cr<sup>4+</sup>:YAG crystal with high damage threshold, low cost, and simplicity is widely used in passively Q-switched lasers. Another advantage of Cr<sup>4+</sup>:YAG crystal is that self-Q-switched laser materials can be fabricated by co-doping Cr<sup>4+</sup> ions and lasants in YAG host crystal. Cr,Nd:YAG and Cr,Yb:YAG self-Q-switched lasers have been demonstrated [4–6]. Efficient laser operation of microchip lasers requires absorbing sufficient pump power with short crystal length; a high concentration microchip laser material is required to realize sub-nanosecond laser operation. Compared with Nd:YAG laser material, Yb:YAG crystal has several advantages such as a long storage lifetime (951 μs) [7], a very low quantum defect (8.6% with pump wavelength of 941 nm and laser wavelength of 1030 nm), resulting in three times less heat generation during lasing than comparable Nd-based laser systems [8], broad absorption bandwidth and less sensitive to laser-diode wavelength specifications [9], a relatively large emission cross section [10] suitable for Q-switching operation, and easy growth of high quality and moderate doping concentration crystals without concentration quenching [11]. Temperature dependent emission cross section of Yb:YAG materials [10] provides another flexible design for efficient operation of cryogenically-cooled Yb:YAG lasers [12]. High power laser-diode pumped Yb:YAG lasers have been demonstrated with different laser resonator configurations such as thin disk lasers [13–15], rod lasers [16], microchip lasers [17, 18] and slab lasers [19]. Passively Q-switched Yb:YAG laser with Cr<sup>4+</sup>:YAG crystal as saturable absorber was firstly demonstrated by using Ti:sapphire laser as pump source [20]. Chromium and ytterbium co-doped YAG (Cr,Yb:YAG) crystals have been grown successfully and optical properties of these self-Q-switched laser materials have been

investigated [21, 22]. The self-Q-switched Cr,Yb:YAG laser was firstly demonstrated by using a Ti:sapphire laser as pump source [6]. Laser-diode pumped Cr,Yb:YAG microchip laser with pulse width of 440 ps, peak power over 53 kW has been demonstrated [23]. However, owing to co-doping of chromium ions with Yb ions into YAG host, the fluorescence lifetime decreases with increase of Cr concentration [22]. And there is strong absorption (about 60% of that around 1  $\mu\text{m}$ ) of pump power by  $\text{Cr}^{4+}$  ions at pump wavelength (around 940 nm) owing to the broad absorption spectrum of  $\text{Cr}^{4+}$ :YAG from 800 nm to 1300 nm [24, 25]. The absorbed pump power threshold is high due to the high intracavity loss induced by the defects introducing Cr ions into Cr,Yb:YAG crystal for compact Cr,Yb:YAG microchip laser. The undesirable absorption at pump wavelength of 940 nm for Cr,Yb:YAG self-Q-switched laser crystal limits the laser performance and Cr,Yb:YAG self-Q-switched lasers even cannot lase with high Cr concentration [22]. Recently, enhancement of Cr,Yb:YAG self-Q-switched lasers by bonding Yb:YAG crystal and ceramic has been demonstrated [26, 27]. Slope efficiency of 25% and optical-to-optical efficiency of 18.5% have been obtained in these lasers. Therefore, Yb:YAG/Cr,Yb:YAG self-Q-switched laser provides an effective way to generate efficient laser oscillation for compact and robust Cr,Yb:YAG self-Q-switched lasers.

In this paper, enhanced performance of Cr,Yb:YAG self-Q-switched microchip lasers by sandwiching Cr,Yb:YAG crystal between Yb:YAG crystal and output coupling mirror has been investigated. Highly efficient Yb:YAG/Cr,Yb:YAG self-Q-switched microchip lasers have been demonstrated for the first time to our best knowledge. The effect of the transmission of output coupler ( $T_{oc}$ ) on the enhanced performance of Yb:YAG/Cr,Yb:YAG self-Q-switched microchip lasers has been studied and found that there is an optimum  $T_{oc}$  for best laser performance of Yb:YAG/Cr,Yb:YAG microchip lasers. Slope efficiency of 38% and optical-to-optical efficiency of 32% have been achieved under high pump power intensity. The stable periodical laser pulse trains have been observed at different pump power levels owing to the multi-longitudinal mode oscillation of Yb:YAG/Cr,Yb:YAG self-Q-switched microchip lasers.

## 2. Experimental setup

The schematic diagram of experimental setup for laser-diode pumped Yb:YAG/Cr,Yb:YAG self-Q-switched microchip lasers by bonding Yb:YAG crystal and Cr,Yb:YAG crystal together is shown in Fig. 1. A plane-parallel 1.2-mm-thick Yb:YAG crystal plate doped with 10 at.%  $\text{Yb}^{3+}$  ions was used as gain medium to absorb major portion of the pump power. One surface of the Yb:YAG crystal was coated with anti-reflection at 940 nm and highly reflection at 1030 nm to act as a cavity mirror of the laser. The other surface was coated with anti-reflection at 1030 nm to reduce the intracavity loss. One uncoated 0.5-mm-thick Cr,Yb:YAG crystal plate was attached together to Yb:YAG crystal plate. The Cr,Yb:YAG crystal conducted self-Q-switched laser oscillation and further absorbed residual pump power for enhancing laser performance. The doping concentrations of  $\text{Yb}^{3+}$  and Cr ions in Cr,Yb:YAG crystal are 10 at.%, and 0.025 at.%, respectively. The initial transmission of 0.5-mm-thick Cr,Yb:YAG crystal was estimated to be 94% by measuring the absorption spectrum of Cr,Yb:YAG around 1  $\mu\text{m}$ . Several 2-mm-thick BK7 glass plane-parallel mirrors with different transmissions ( $T_{oc}$ ) from 5% to 60% at 1030 nm were used as output couplers. The mechanically bonded Yb:YAG/Cr,Yb:YAG crystal plates were held together with plane-parallel output coupling mirror between two copper blocks. The cavity length is 1.8 mm by considering the coating thickness. A high-brightness 940 nm laser-diode with a 1  $\mu\text{m} \times 50 \mu\text{m}$  emitting cross section was used as the pump source. The fast-axis divergence angle of the laser-diode was shaped to 10 degrees with a micro-lens at the output facet of laser-diode. Two lenses with 8-mm focal length were used to collimate and focus the pump beam on the Yb:YAG crystal rear surface, the footprint of the focus spot was measured to be 80  $\times$  80  $\mu\text{m}^2$ . The Cr,Yb:YAG self-Q-switched microchip lasers enhanced by bonding Yb:YAG crystal operated at room temperature without active cooling. The laser emitting spectra were measured with ANDO (AQ6317B) optical spectral analyzer. Average output power and pulse

characteristics were measured with a Thorlabs PM200 power meter and 400 MHz Tektronix digital oscilloscope, respectively.

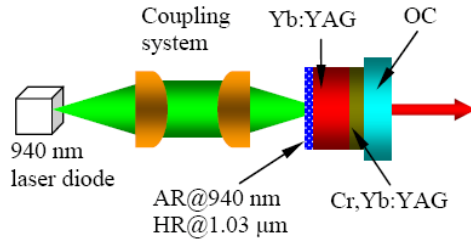


Fig. 1. Schematic diagram of experimental setup for laser-diode pumped Yb:YAG/Cr,Yb:YAG self-Q-switched microchip laser. OC is the output coupler.

### 3. Results and discussion

Coating damage on the output coupler was occurred when the transmission of output coupler,  $T_{oc}$ , was equal to or less than 20% at high pump power levels owing to the high intracavity intensity with low transmissions of output coupler. Therefore, transmission of output coupler greater than 20% was used for investigating the enhanced performance of Yb:YAG/Cr,Yb:YAG self-Q-switched microchip lasers. The absorbed pump power of Yb:YAG/Cr,Yb:YAG microchip lasers was obtained by measuring the incident pump power after coupling optics and residual power after Yb:YAG/Cr,Yb:YAG crystals under no lasing condition for different pump power levels. The pump power absorption efficiency of Yb:YAG/Cr,Yb:YAG crystals was measured to be about 78%. The average output power of Yb:YAG/Cr,Yb:YAG self-Q-switched microchip lasers as a function of the absorbed pump power for different output couplings ( $T_{oc}$ ) is shown in Fig. 2, together with the optical-to-optical efficiency as a function of the absorbed pump power for  $T_{oc} = 50\%$ . The absorbed pump power thresholds are 0.23, 0.24, 0.27, and 0.39 W for  $T_{oc} = 30, 40, 50,$  and  $60\%$ , respectively. The absorbed pump power threshold increases with transmission of the output coupler because the intracavity loss is proportional to  $T_{oc}$ . The average output power increases nearly linearly with the absorbed pump power when the absorbed pump power is well above the pump power threshold for  $T_{oc} = 30, 40, 50,$  and  $60\%$ . However, the average output power tends to increase slowly when the absorbed pump power is higher than 2.1 W for different output couplings. The slope efficiencies were measured to be about 34, 36, 38, and 31% for  $T_{oc} = 30, 40, 50,$  and  $60\%$ , respectively. There is an optimum transmission of output coupler,  $T_{oc} = 50\%$ , for best laser performance obtained in laser-diode pumped Yb:YAG/Cr,Yb:YAG microchip lasers. Maximum average output power of 0.8 W was achieved at absorbed pump power of 2.5 W for  $T_{oc} = 50\%$ , corresponding optical-to-optical efficiency of 32% was obtained. The optical-to-optical efficiency increases with the absorbed pump power and the highest optical-to-optical efficiency is achieved when the absorbed pump power is 1.7 W. Then the optical-to-optical efficiency tends to decrease with further increase of the pump power when the absorbed pump power is higher than 1.7 W. The saturation of the optical-to-optical efficiency may be caused by the fully depletion of population at ground state of Yb:YAG crystal and Cr,Yb:YAG crystal under high pump power intensity when the absorbed pump power is higher than 1.7 W. The decrease of the optical-to-optical efficiency with further increase of pump power may be caused by the thermal effect of Yb:YAG crystal under high pump power intensity. Laser performance of Yb:YAG/Cr,Yb:YAG self-Q-switched microchip lasers is better than those obtained in laser-diode pumped monolithic Cr,Yb:YAG self-Q-switched microchip laser [23], and Yb:YAG/Cr,Yb:YAG self-Q-switched lasers with 70-mm-long plano-concave cavity [26]. Enhanced performance of Yb:YAG/Cr,Yb:YAG self-Q-switched microchip lasers was attributed to the high pump power intensity used in the laser experiments and increase of the length of Yb:YAG crystal from 1 mm [26] to 1.2 mm. The pump power intensity used in microchip laser is about  $40 \text{ kW/cm}^2$ , which is about 3 times

higher than that used in Ref [26]. Therefore, the absorption of the pump power increases and the effective inversion population increases under high pump power intensity.

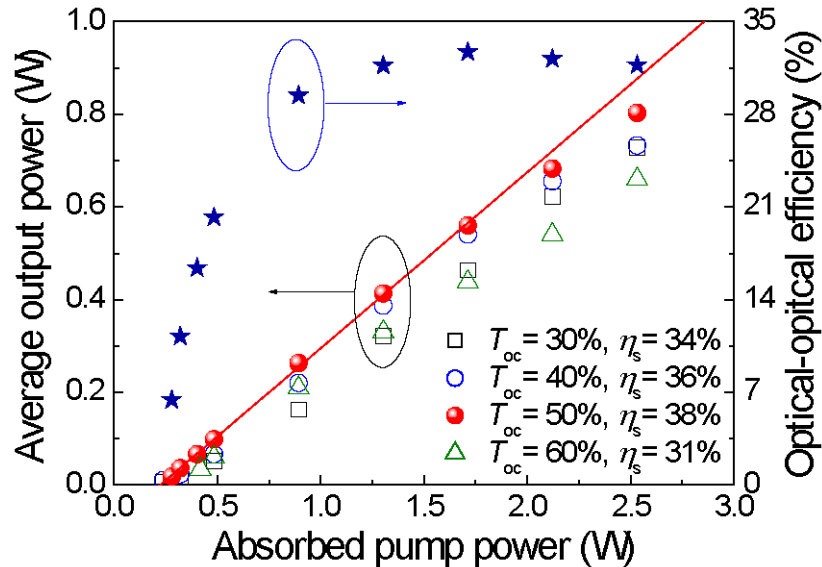


Fig. 2. Average output power of Yb:YAG/Cr,Yb:YAG self-Q-switched microchip lasers as a function of the absorbed pump power for different transmission of output coupler,  $T_{oc}$ ; together with the optical-to-optical efficiency as a function of the absorbed pump power for  $T_{oc} = 50\%$ . The line shows the linearly fitting of experimental data for  $T_{oc} = 50\%$ .

The measured laser emitting spectra show that the Yb:YAG/Cr,Yb:YAG self-Q-switched microchip lasers oscillate in multi-longitudinal-mode for different output couplings. And the number of longitudinal modes increases with the absorbed pump power. Figure 3 shows the laser emitting spectra of Yb:YAG/Cr,Yb:YAG self-Q-switched microchip lasers with  $T_{oc} = 50\%$  under different absorbed pump power levels. Three longitudinal modes oscillated when the absorbed pump power was kept below 1.8 W. The wavelengths and intensities of three longitudinal modes varied with the absorbed pump power, as shown in Fig. 3(a) and Fig. 3(b). Four longitudinal modes were observed when the absorbed pump power was higher than 1.8 W, as shown in Fig. 3(c). The separation between each mode was measured to be about 0.44 and 0.66 nm, wider than the free spectral range  $\Delta\lambda_c = 0.171$  nm in the laser cavity filled with gain medium predicted by  $\Delta\lambda_c = \lambda^2/2L_c$  [28], where  $L_c$  is the optical cavity length and  $\lambda$  is laser wavelength. The wide separation between longitudinal modes was attributed to the combination mode selection from intracavity tilted etalon effect of the Cr,Yb:YAG, Yb:YAG thin plates and output coupler mirror. The potential output longitudinal modes were selected by the combined etalon effect of the 0.5-mm-thick Cr,Yb:YAG, 1.2-mm-thick Yb:YAG thin plate and 2-mm-thick BK7 glass mirror as an intracavity etalon [28]. Figure 3(d) shows the possible selected modes by the combining etalon effect of 1.2-mm-thick Yb:YAG, 0.5-mm-thick Cr,Yb:YAG and 2-mm-thick BK7 glass, which are in good agreement with the experimental results as shown in Fig. 3(b) at the absorbed pump power of 1.3 W. The resonant modes at 1029.95 nm, four times of free spectral range (0.171 nm) away from the main mode centered at 1030.6 nm, will oscillate preferably because the wavelength of these modes is very close to the high transmittance of the combined transmittance product and the highest gain of Yb:YAG crystal centered at 1029.7 nm. The resonant mode will oscillate at 1029.48 nm due to the asymmetric gain profile centered at 1029.7 nm of Yb:YAG crystals. At high pump power levels, besides the oscillation of the main mode depleting the inversion population and suppressing the oscillation of the resonant modes close to it, the local temperature rise induced by the pump power changes the transmittance of the etalons.

Therefore, the relative gain and loss for different resonant modes are varied, which determine the wavelengths and number of the longitudinal modes oscillating.

The laser emitting wavelengths shift to longer wavelength with the absorbed pump power owing to the temperature dependent emission spectra of Yb:YAG and Cr,Yb:YAG crystals [10, 29]. The temperature of Yb:YAG and Cr,Yb:YAG crystals increases with the absorbed pump power, emission spectra of Yb:YAG and Cr,Yb:YAG crystals shift to longer wavelength with temperature, laser emitting wavelengths shift to longer wavelength accordingly.

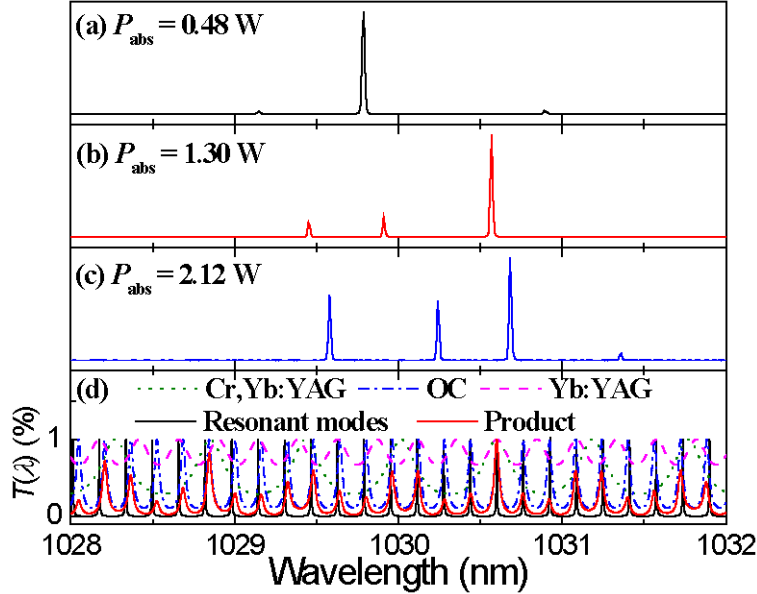


Fig. 3. Typical laser emitting spectra of Yb:YAG/Cr,Yb:YAG self-Q-switched microchip laser under different pump power levels for  $T_{\text{oc}} = 50\%$ , (a)  $P_{\text{abs}} = 0.48 \text{ W}$ , (b)  $P_{\text{abs}} = 1.3 \text{ W}$ , (a)  $P_{\text{abs}} = 2.12 \text{ W}$ ; (d) Transmittance curves of 0.5-mm-thick Cr,Yb:YAG, 1.2-mm-thick Yb:YAG, 2-mm-thick BK7 glass output coupler (OC), and their transmittance product. Resonant modes are also plotted for illustration.

Some typical laser pulse trains of Yb:YAG/Cr,Yb:YAG self-Q-switched microchip laser at different pump power levels for  $T_{\text{oc}} = 50\%$  are shown in Fig. 4(a–c). The laser pulse trains exhibit periodical pulsation at different pump power levels owing to the multi-longitudinal modes oscillation. The repetition rate increases with the absorbed pump power. Although Yb:YAG/Cr,Yb:YAG self-Q-switched microchip laser oscillated in three-longitudinal modes when the absorbed pump power was kept below 1.8 W, the intensities and wavelengths of each longitudinal mode were different because the modes competed for the gain. Therefore, the laser pulse trains exhibited different characteristics. At low pump power, two weak modes oscillated besides the main mode, the modulation of laser pulse trains was weak, and period-7 pulsation was observed, as shown in Fig. 4(a). The intensities of other side modes increased with absorbed pump power, the modulation of pulse trains became stronger, and the laser pulse trains exhibited period-3 pulsation, as shown in Fig. 4(b). The laser pulse trains exhibited period-4 pulsation when the laser oscillated at four-longitudinal modes, as shown in Fig. 4(c). The oscilloscope pulse profile at the absorbed pump power of 2.5 W for  $T_{\text{oc}} = 50\%$  is shown in Fig. 4(d). The Yb:YAG/Cr,Yb:YAG self-Q-switched laser pulse with pulse energy of 12.4  $\mu\text{J}$  and pulse width (FWHM) of 1.68 ns was measured. Therefore, the peak power of self-Q-switched laser was estimated to be 7.4 kW.

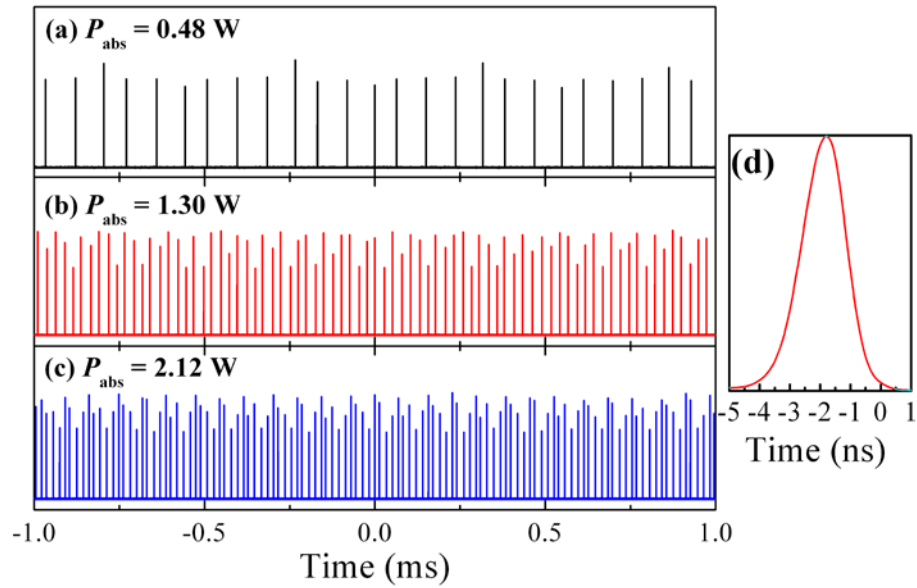


Fig. 4. Laser pulse trains of Yb:YAG/Cr,Yb:YAG self-Q-switched microchip laser at different pump power levels for  $T_{oc} = 50\%$ , (a)  $P_{abs} = 0.48$  W, (b)  $P_{abs} = 1.3$  W, (c)  $P_{abs} = 2.12$  W; and (d) laser pulse profile with 1.68 ns pulse width, pulse energy of 12.4  $\mu$ J, and peak power of 7.4 kW.

Figure 5 shows the pulse repetition rate and pulse width of Yb:YAG/Cr,Yb:YAG self-Q-switched microchip laser as a function of the absorbed pump power for  $T_{oc} = 50\%$ . The repetition rate increases linearly with the absorbed pump power. However, the increase ratio of repetition rate with absorbed pump power is different when the absorbed pump power is lower than 1 W comparing with that at high absorbed pump power levels. The increase ratio of repetition rate is 38 kHz/W when the absorbed pump power is lower than 1 W, while it is 22 kHz/W when the absorbed pump power is higher than 1 W. This may be caused by the strong multi-longitudinal modes competition at high pump power level. The pulse width (FWHM) nearly keeps constant at different absorbed pump power levels when the absorbed pump power is higher than 1 W because  $\text{Cr}^{4+}$  ions in Cr,Yb:YAG crystal was fully bleached under high intracavity laser intensity. Figure 6 shows the pulse energy and peak power of Yb:YAG/Cr,Yb:YAG self-Q-switched microchip laser as a function of the absorbed pump power for  $T_{oc} = 50\%$ . Pulse energy and peak power increase with the absorbed pump power and tend to be saturated when the absorbed pump power is higher than 2 W. The pulse width, pulse energy, and peak power are nearly independent of the pump power for different transmission of output couplers when the absorbed pump power is higher than 2 W. According to the passively Q-switched laser theory [28, 30, 31], the pulse energy and the pulse width are determined by the initial transmission of saturable absorber and the parameters of the laser cavity, and do not depend on the pump power when the pump power is above the pump power threshold, so is the peak power.

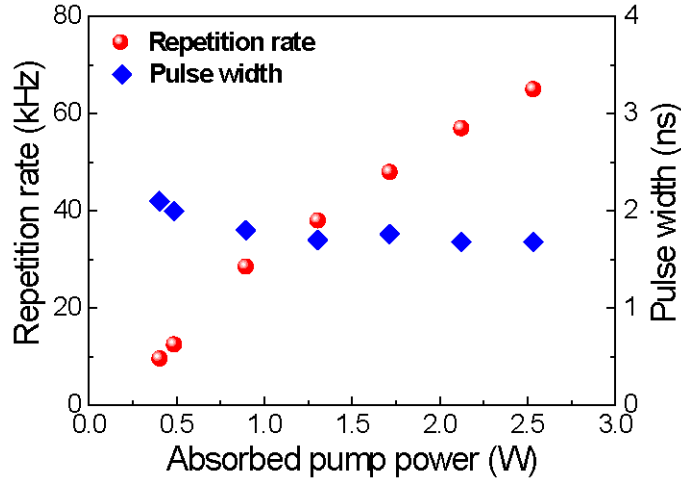


Fig. 5. Pulse repetition rate and pulse width of Yb:YAG/Cr,Yb:YAG self-Q-switched microchip laser as a function of the absorbed pump power for  $T_{oc} = 50\%$ .

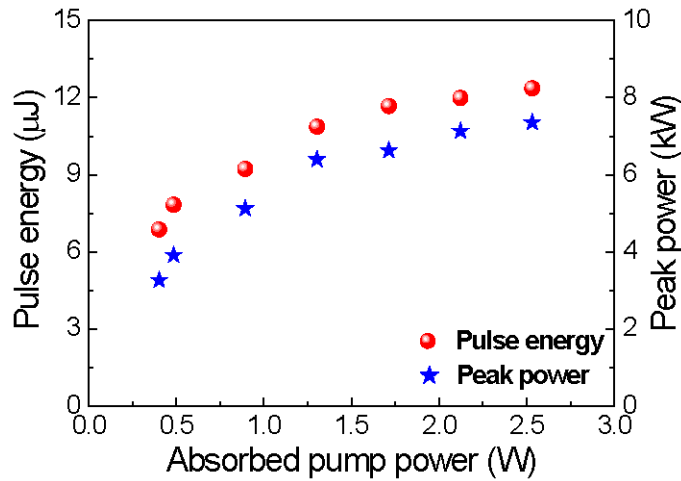


Fig. 6. Pulse energy and peak power of Yb:YAG/Cr,Yb:YAG self-Q-switched microchip laser as a function of the absorbed pump power for  $T_{oc} = 50\%$ .

Figure 7 shows the pulse characteristics such as pulse energy, peak power, repetition rate ( $f$ ), pulse width (FWHM), average output power ( $P_{out}$ ), and optical-to-optical efficiency ( $\eta_{o-o}$ ) of Yb:YAG/Cr,Yb:YAG self-Q-switched microchip lasers as a function of transmission of output coupler ( $T_{oc}$ ) when the absorbed pump power was set to 2.5 W. Pulse energy and peak power increase with  $T_{oc}$  until  $T_{oc} = 50\%$  and then decrease with  $T_{oc}$ . Pulse width keeps constant with  $T_{oc}$  until  $T_{oc} = 50\%$  and then increases with  $T_{oc}$ . Repetition rate of over 60 kHz of Yb:YAG/Cr,Yb:YAG self-Q-switched microchip lasers was obtained for different output couplings under high pump power intensity. Repetition rate decreases with  $T_{oc}$  until  $T_{oc} = 50\%$  and then increase a little at  $T_{oc} = 60\%$ . The increase of repetition rate at  $T_{oc} = 60\%$  may be caused by the thermal lens effect induced by the less efficient laser performance of Yb:YAG/Cr,Yb:YAG microchip laser. The thermal lens effect becomes stronger at high pump power. The pump beam diameter decreases, so the pump power intensity increases. Therefore, the repetition rate of Yb:YAG/Cr,Yb:YAG self-Q-switched microchip laser increases. Average output power and optical-to-optical efficiency increase with  $T_{oc}$  until  $T_{oc} = 50\%$  and then decrease with  $T_{oc}$ . There is an optimum  $T_{oc}$  for achieving best laser performance



of laser-diode pumped Yb:YAG/Cr,Yb:YAG self-Q-switched microchip lasers. Based on the results of laser-diode pumped Yb:YAG/Cr,Yb:YAG self-Q-switched microchip lasers under high pump power intensity, highly efficient, high pulse energy, high peak power Yb:YAG/Cr,Yb:YAG self-Q-switched microchip lasers can be constructed by using thin Cr,Yb:YAG crystal doped with high Cr concentration.

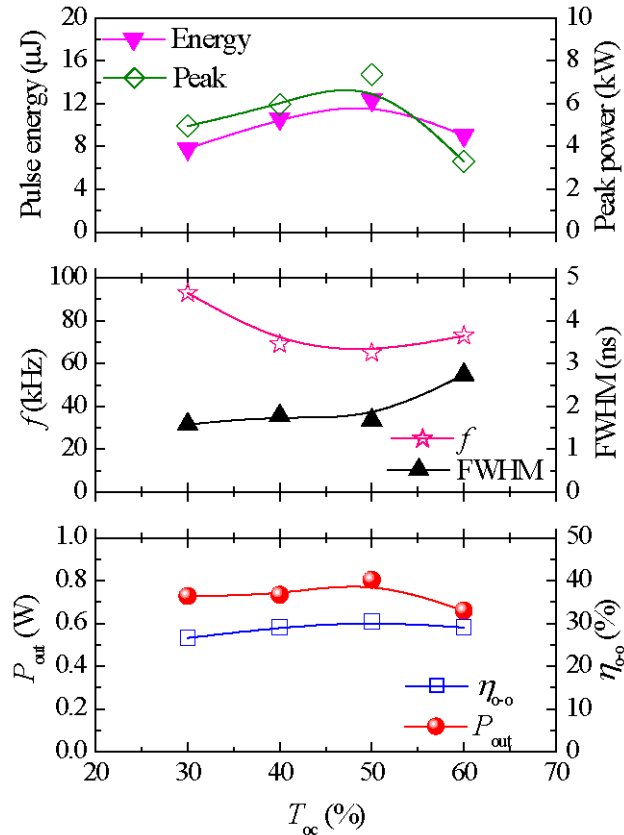


Fig. 7. Pulse characteristics such as pulse energy, peak power, pulse repetition rate, pulse width, average output power, and optical-to-optical efficiency of Yb:YAG/Cr,Yb:YAG self-Q-switched microchip laser as a function of transmission of output coupler when the absorbed pump power was set to 2.5 W. The solid lines were used to illustrate the variation tendency of pulse characteristics with  $T_{oc}$ .

#### 4. Conclusions

Highly efficient Yb:YAG/Cr,Yb:YAG self-Q-switched microchip lasers enhanced by bonding Yb:YAG crystal have been demonstrated for the first time. Best laser performance of Yb:YAG/Cr,Yb:YAG self-Q-switched microchip lasers was achieved with 50% transmission of output coupler. Maximum output power of 0.8 W was obtained when the absorbed pump power of 2.5 W was applied; corresponding optical-to-optical efficiency of 32% was achieved with respect to the absorbed pump power. Slope efficiency of 38% was achieved with  $T_{oc} = 50\%$ . Laser pulses with pulse energy of 12.4  $\mu\text{J}$ , pulse width of 1.68 ns and peak power of 7.4 kW were achieved. Repetition rate of over 60 kHz was obtained. The lasers oscillate in multi-longitudinal-mode and the number of longitudinal modes increases with the pump power. Transmission of output coupler has great impact on the pulse energy, peak power and repetition rate, and has little effect on the pulse width of Yb:YAG/Cr,Yb:YAG self-Q-switched microchip lasers. The enhanced performance of Yb:YAG/Cr,Yb:YAG self-Q-

switched microchip lasers can be further improved by using thin Cr,Yb:YAG crystal doped with high Cr concentration.

### **Acknowledgments**

This work was supported by the National Natural Science Foundation of China (61275143), the Program for New Century Excellent Talents in University (NCET-09-0669), the Fundamental Research Funds for the Central Universities (2010121058), and the Ph.D. Programs Foundation of Ministry of Education of China (20100121120019).